Nanospintronics: when spintronics meets single electron physics

2007 J. Phys.: Condens. Matter 19 165222

(http://iopscience.iop.org/0953-8984/19/16/165222)

IOP PUBLISHING JOURNAL OF PHYSICS: CONDENSED MATTER

J. Phys.: Condens. Matter **19** (2007) 165222 (22pp) doi:10.1088/0953-8984/19/16/165222

Nanospintronics: when spintronics meets single electron physics

Pierre Seneor, Anne Bernand-Mantel and Frédéric Petroff

Unité Mixte de Physique CNRS/Thales, 91767 Palaiseau Cedex, France
and
Université de Paris-Sud 11, 91405 Orsay Cedex, France

E-mail: pierre.seneor@thalesgroup.com

Received 22 September 2006, in final form 27 November 2006
Published 6 April 2007
Online at stacks.iop.org/JPhysCM/19/165222

Abstract

As spintronics goes nano, new phenomena are predicted resulting from the interplay between spin dependent transport and single electron physics. The long term goal of manipulating spins one by one would open a promising path to quantum computing. Towards this end, there is an ever-growing effort to connect spin tanks (i.e. ferromagnetic leads) to smaller and smaller objects in order to study spintronics in reduced dimensions. As the dimensions are reduced, spin dependent transport is predicted to interplay with quantum and/or single electron charging effects. We review experiments and theories on the interplay between Coulomb blockade and spin properties (namely magneto-Coulomb effects) in structures where a single nano-object is connected to ferromagnetic leads. We then discuss briefly future directions in the emerging field of nanospintronics towards quantum dots, carbon nanotubes and single molecule magnets.

(Some figures in this article are in colour only in the electronic version)

Contents

1. Introduction to Coulomb blockade

1.1. Principle

Let us consider a structure where a small conductive dot or island (either metallic or semiconducting, organic or inorganic) is linked to two electrodes by two tunnel junctions. The simplest example is a metallic nanoparticle embedded into a tunnel junction as shown in figure 1(A). The tunnelling of a charge from an electrode to this small dot requires a charging energy $E_C = e^2/2C_T$ to be overcome, where $C_T = C_1 + C_2$ is the total capacitance of the dot and $C_{i=1,2}$ relates to each junction. Using a simple picture, this translates the extra energy due to the electrostatic Coulomb repulsion that appears when trying to add another electron to the closely packed electron cloud of the nanoparticle. At low enough voltage and temperature, where $eV, k_BT \ll E_C$, this charging energy introduces a gap for electron tunnelling and the system is in the so-called Coulomb blockade regime. Sequential tunnelling through the dot is suppressed and the current vanishes (only very small leakage currents corresponding to higher order tunnelling processes can be observed [1]). The dot becomes unblocked when enough energy is supplied by the applied voltage for an electron to move into (or out of) it as shown in figure 1(B). The incoming electron adds a new charging energy so that another electron is forbidden to enter the dot and has to wait for this electron to leave first. This gives rise to a single electron current flowing through the dot. As the applied voltage is increased a second (third, fourth, ...) threshold is reached, enabling a two (three, four, ...) electron current to flow, giving rise to the well known Coulomb staircase in the $I(V)$ curve (see figure 1(C)). This behaviour is well explained by the 'orthodox' theory of Coulomb blockade in single electron devices [2–4].

1.2. Conditions of observation

Two conditions are required to observe this effect. First, the tunnel resistance between the dot and either of the two electrodes must be larger than the quantum resistance $R_q = h/e^2 \simeq 26\ \mathrm{k}\Omega$. This follows from the uncertainty principle. If the resistance is lower than R_q, the electron wavefunction cannot be localized on the dot and the number of electrons fluctuates on it even in the Coulomb blockade regime. The second condition concerns the ratio of the charging energy to the temperature. The charging energy has to be large compared to the thermal energy ($E_C \gg k_BT$). Otherwise, electrons can be heated up to tunnel into the dot and Coulomb blockade is suppressed. As an example, if the dot is assumed to be an isolated sphere, its capacitance can be written $C = 2\pi\epsilon_r\epsilon_0 d$, where d is the dot diameter and ϵ_r the embedding matrix dielectric constant. Thinking about potential applications, for reliable room temperature Coulomb blockade in the case of an Al_2O_3 matrix ($\epsilon_r = 9$) one finds $d \ll 6$ nm, requiring the ability to contact dots with diameter of around or less than 1 nm. However, with dielectric constants as low as $\epsilon_r \simeq 2$, organic compounds used as matrices would provide a very interesting consistent solution to room temperature Coulomb blockade, gaining almost a factor of five in the dot size. However, reliable techniques to connect dots with diameters of a few

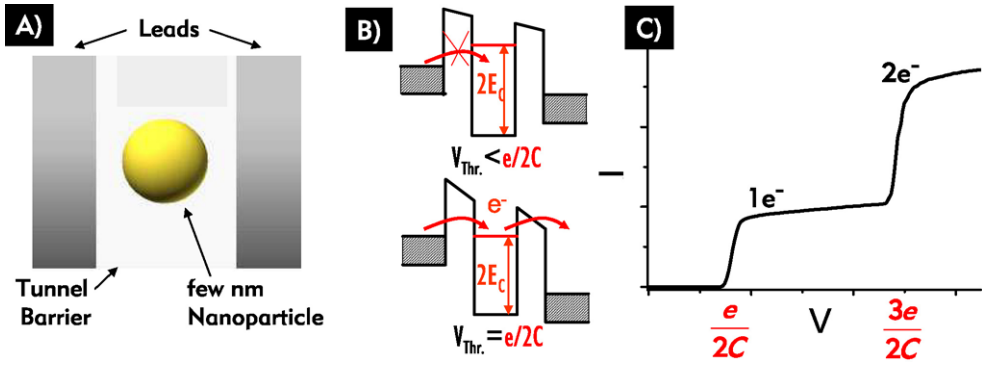

Figure 1. (A) Schematic representation of the type of double junction studied: a nano-object is linked to two leads via two tunnel junctions. (B) Energy diagram representation of the Coulomb blockade effect showing the blocked regime (upper panel) and the onset of the single electron current (lower panel). (C) Simulated $I(V)$ curve of an ideal double junction with symmetric capacitances ($C_1 = C_2 = C$) and strongly asymmetric resistances showing Coulomb steps.

nanometres are required. This illustrates the difficulty of getting room temperature Coulomb blockade as the size control of such small structures is still a technological challenge, not taking into account the almost necessary addition of ferromagnetic materials for spintronics purposes.

1.3. Influence of the background charge

The background (or induced) charge Q_0 corresponds to the effective electric environment experienced by the electrons on the dot. In most of the theories this charge is taken to be null, which means that at zero bias voltage the sample is in the middle of the Coulomb gap. The energy E_C has to be overcome in negative or positive bias to charge the dot, the full gap being $2E_C$ (see figure 6). However, in real experiments Q_0 will almost always end up with a finite value, shifting the gap. This value often changes while applying a bias voltage on the system as electrons may become trapped or untrapped nearby the dot. Also, most of the time, warming up and cooling down the system will change this value. As it is somehow equivalent to an unknown fixed voltage applied on the gate, in single electron transistors (SETs) it can be easily compensated. In double junctions, one has no gate to compensate. In figure 2, we present some aspects of the curve zoology one can expect when working on double junctions [5]. The ideal case with sharp steps corresponds to $C_1 < C_2$, $R_1 \ll R_2$ and $Q_0 = 0$ as shown in figure 2(A) (blue curve). However, in most of the nanostructures, especially the ones where a nano-object is placed between two identical leads, we will find the opposite situation. This follows the intuition that if the nano-object is closer to, say, lead 2, because the capacitance and the resistance have opposite variations as a function of the dot to lead distance, we obtain $C_1 < C_2$ and $R_1 > R_2$. For $Q_0 = 0$, the first steps are then transformed into slopes as seen in figure 2(A) (black curve). In figure 2(B), we show what is expected in this case ($C_1 < C_2$, $R_1 \gg R_2$) for two different Q_0. The inset curves are vertical sections of diagram C in figure 2. For Q_0 high enough, one sharp step is restored (as the vertical section crosses the dashed line of the diagram while leaving the gap), but the Coulomb gap is reduced. If $Q_0 = \pm 0.5e$ the gap is fully suppressed. In fact, very often the condition will be resumed to $C_1 \lesssim C_2$ and $R_1 \gg R_2$ as the capacitance varies much more slowly than the exponential dependence of the tunnel resistance. This will give an almost square shape for the parallelograms in the diagram of figure 2(C). Hence, any non-integer finite value of Q_0/e will bring $I(V)$ curves with one

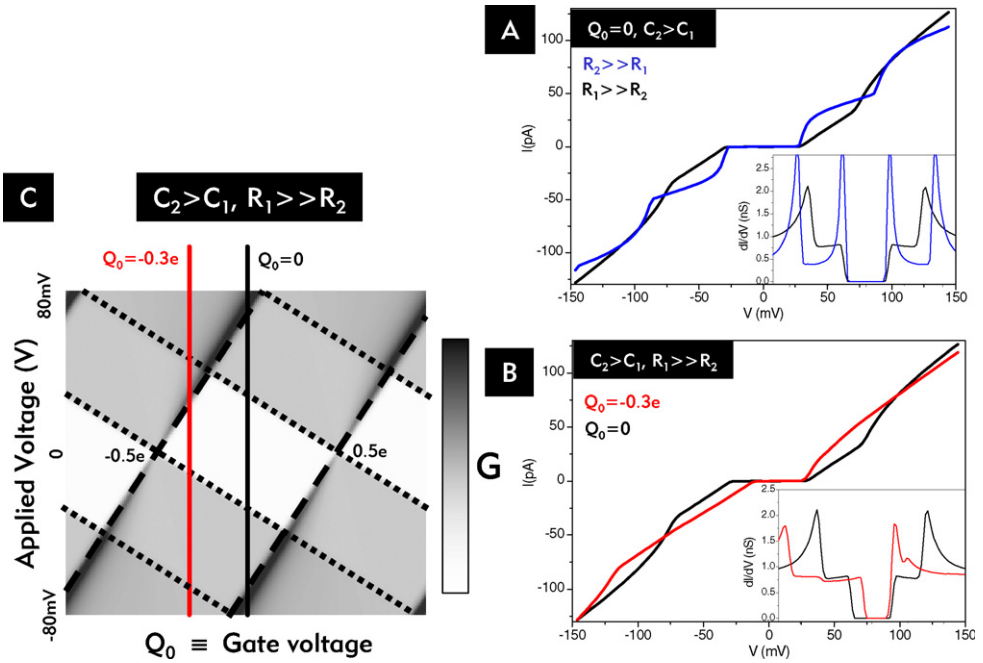

Figure 2. (A) Simulated $I(V)$ curves (inset $\mathrm{d}I/\mathrm{d}V(V)$ curves) at $Q_0 = 0$ showing the different parameters leading to sharp Coulomb steps ($C_1 < C_2$, $R_1 \ll R_2$, blue curve) or slow slopes ($C_1 < C_2$, $R_1 \gg R_2$, black curve). (B) Simulated $I(V)$ curves (inset $\mathrm{d}I/\mathrm{d}V(V)$ curves) at two different Q_0 states showing either two slopes ($Q_0 = 0$, black curve) or a sharp step and a slope ($Q_0 = -0.3e$ red curve). The parameters are $C_1 < C_2$, $R_1 \gg R_2$. (C) Grey scale plot of the conductance versus applied voltage V and background charge Q_0 (equivalent to a gate voltage). The $\mathrm{d}I/\mathrm{d}V(V)$ curves of the top right figure correspond to sections of the diagram following the vertical red line ($Q_0 = -0.3e$) and black line ($Q_0 = 0$). Each time the vertical section crosses a dashed line (dotted line) a sharp peak (broad peak) is found. The fixed parameters for all the curves are $C_2 = 2.5C_1 = 2.75$ aF, and $R_{\max} = 12R_{\min} = 850$ MΩ. Curves were simulated using rate equations and following the orthodox theory.

sharp step and one slow slope. This should be observed in most of the nanostructure elaborated from nano-objects. A difference arises in the case of gated systems. There, one can apply a very small source–drain voltage while varying the capacitively coupled gate (horizontal cut at $V = 0$ in the diagram of figure 2(C)). What is then observed is a series of very sharp peaks, mostly enlarged by $K_{\mathrm{B}}T$ for weak coupling to the electrodes.

2. Magneto-Coulomb effects

2.1. Early experiments

The interplay between Coulomb blockade and spin dependent tunnelling was first investigated [6, 7] in the 1970s in Ni/SiO_2 granular films called cermets. Below the metallic percolation threshold, these films consist of randomly distributed ferromagnetic nanosized clusters embedded in an insulating matrix. Twenty years later, with the advent of spintronics, these materials regained interest following the report of tunnelling magnetoresistance (TMR) in Co–Al–O granular films [8]. Due to the large thickness of the films (1–2 μm), a huge number of nanosized Co clusters were involved in the tunnelling processes. A step towards simpler structures was made soon after by Schelp *et al* [9] and Dieny *et al* [10], who investigated

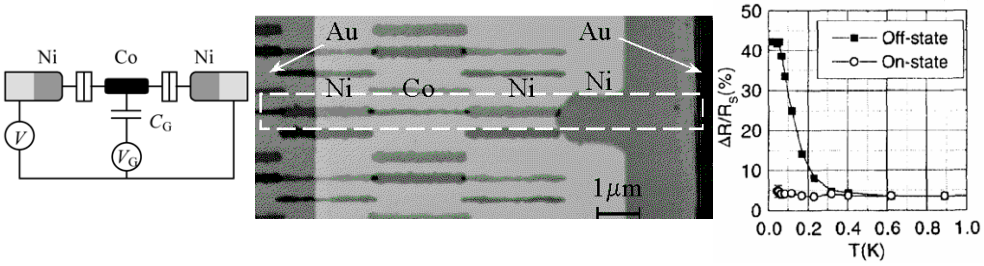

Figure 3. Left panel: schematic diagram of the Ni/Co/Ni SET. Middle panel: AFM micrograph of an Ni/Co/Ni SET delimited by the rectangle in a dashed line. The Co dot is 15 nm thick and has an area of $0.15 \times 2.5\ \mu m^2$ with a tunnel junction surface of about $0.02\ \mu m^2$. The charging energy $E_C = e^2/2C$ is in the 50–100 μeV range. The two black spots at the Ni/Co interfaces are the tunnel junctions. The gate is on the rear surface of the sample. Right panel: magnetoresistance versus temperature in the on and off states (controlled by the gate), showing an MR enhancement at low temperature in the blocked regime. Figures are adapted from [12–14].

Co/X (X = SiO_2, Al_2O_3) granular multilayers with respectively one or several 2D arrays of Co clusters. A different approach was initiated at the same period by Ootuka *et al* [11] with the development of a mesoscopic ferromagnetic single electron transistor as further described below.

2.2. TMR in the Coulomb gap; effect of higher order processes

The first observation of the interplay between Coulomb blockade and spin dependent tunnelling was the measurement of enhanced TMR (see below). The Ootuka group measured enhanced magnetoresistance (MR) in a series of Ni/NiO/Co small tunnel junctions in the Coulomb blockade regime [11]. They further created [15] a Ni/NiO/Co/NiO/Ni ferromagnetic single electron transistor (F-SET) see figure 3. Defined by electron beam lithography, the Co dot was 15 nm thick and had an area of $0.15 \times 2.5\ \mu m^2$ with a tunnel junction surface of about $0.02\ \mu m^2$. They found charging energies $E_C = e^2/2C$ of such dots to be within 50–100 μeV, limiting the Coulomb blockade observation range to very low temperatures below liquid He. Enhanced MR of 40% was obtained at 20 mK in the blocked regime while only 3.8% could be observed outside of the Coulomb blockade regime. They related this effect to the occurrence of higher order tunnelling processes in the blockade regime, where sequential tunnelling is exponentially suppressed. The variation of the spin dependent tunnelling resistance between the dot and an electrode was expected to have a stronger influence in this higher order tunnelling process. This experiment was quickly followed by other experiments [16–18] and theoretical modelling in the cotunnelling regime where TMR enhancement was predicted (while not explaining the factor of 10 observed by Ootuka *et al*) for either granular films [19] or double tunnel junctions [20–22]. This cotunnelling regime, originally discussed by [1], is a second order tunnelling process that occurs at low voltage and temperature when Coulomb blockade forbids sequential tunnelling through the double junction. It can be either elastic or inelastic. In the elastic case, the same electron tunnels through the system, whereas in the inelastic case the process is equivalent to the probability of two charges simultaneously tunnelling in and out of the central dot. Being a higher order process, it is less effective and currents are much smaller than in the sequential tunnelling regime. According to [21], at zero applied bias, in the cotunnelling regime the resistance can be written

$$R_\sigma^{\mathrm{cot}} \approx \frac{3e^2}{2h}[R_T^\sigma]^2 (E_C/kT)^2, \qquad (E_C \gg kT) \tag{1}$$

whereas at higher temperatures it is replaced by the one for thermally assisted sequential tunnelling

$$R_\sigma^{\text{seq}} \approx 2R_T^\sigma(1 + E_C/3kT), \qquad (kT \gg E_C) \tag{2}$$

where σ stands for the relative antiparallel ($\uparrow\downarrow\uparrow$) or parallel ($\uparrow\uparrow\uparrow$) orientations of the electrode/dot/electrode magnetizations, R_σ is the structure's differential resistance and R_T^σ that of each tunnel junction. In this calculation the dot and electrodes are supposed to be made of the same ferromagnet and the two electrode/dot tunnel junctions have similar capacitance and resistance R_T^σ. With this simple model, one can clearly see that following the intuition, the overall cotunnelling resistance is proportional to the product of the two tunnel resistances whereas that of the sequential regime is proportional to their sum. The TMR in the sequential regime can be written

$$\text{TMR}_{\text{seq}} = \frac{R_{\uparrow\downarrow\uparrow}^{\text{seq}} - R_{\uparrow\uparrow\uparrow}^{\text{seq}}}{R_{\uparrow\uparrow\uparrow}^{\text{seq}}} = \frac{R_T^{\uparrow\downarrow} - R_T^{\uparrow\uparrow}}{R_T^{\uparrow\uparrow}} \tag{3}$$

while that in the cotunnelling regime is

$$\text{TMR}_{\text{cot}} = \frac{(R_{\uparrow\downarrow\uparrow}^{\text{cot}})^2 - (R_{\uparrow\uparrow\uparrow}^{\text{cot}})^2}{(R_{\uparrow\uparrow\uparrow}^{\text{cot}})^2} = \frac{(R_T^{\uparrow\downarrow})^2 - (R_T^{\uparrow\uparrow})^2}{(R_T^{\uparrow\uparrow})^2} \tag{4}$$

$$= 2\text{TMR}_{\text{seq}} + \text{TMR}_{\text{seq}}^2 \tag{5}$$

giving an enhanced TMR in the cotunnelling regime at least equal to twice the TMR in the sequential regime. This enhancement is expected to disappears when sequential tunnelling is restored or in the limit of very high tunnel resistances, where cotunnelling progressively vanishes. Conclusive experimental evidence was recently reported by [23] with TMR increasing from 11% to 24% for a bidimensional array of CoFe clusters embedded in a CoFe/Al_2O_3/CoFe tunnel junction. Also, it is worth mentioning that an even higher TMR enhancement was predicted at very low temperature in the strong tunnelling regime by taking into account higher order processes [24].

2.3. Magnetic field induced magneto-Coulomb shift and oscillations

While the resistance of a SET is known for oscillating with the gate voltage (see section 1.3), Coulomb oscillations versus applied magnetic field were also found by the Ootuka group in Ni/Co/Ni [13, 15], Co/Ni/Co and Al/Co/Al SETs [25, 26] (see the diagrams in figure 4). This oscillation was explained by a shift of the electrochemical potential of a ferromagnet when a magnetic field is applied. In a magnetic field, the energy of an electron changes by $\pm(1/2)g\mu_B\mu_0 H$ due to the Zeeman effect, according to its spin (g, μ_B and H are respectively the gyromagnetic ratio, the Bohr magneton and the applied magnetic field). As the ferromagnet has different spin up and spin down density of states at the Fermi energy, a repopulation of the electrons appears as shown in the left panel of figure 4. This results in a shift of the ferromagnet's electrochemical potential of $\Delta\mu = -\frac{1}{2}Pg\mu_B\mu_0 H$, where $P = (D_\uparrow - D_\downarrow)/(D_\uparrow + D_\downarrow)$ is the spin polarization at the Fermi energy using the *full* spin dependent density of states D_σ of the ferromagnet[1]. Let us consider the simple case of the Al/Co/Al SET (see figure 4, bottom right) where the dot is the only ferromagnet. We implicitly suppose that the dot is the middle of the Coulomb gap ($Q_0 = 0$) for $H = 0$. For an applied field, when the shift equals the charging energy $\Delta\mu = E_C$ (that is $\Delta Q_0 = 0.5e$), the dot switches

[1] Care must be taken not to confuse this polarization with the spin polarization extracted from spin dependent tunnelling experiments. For example, the polarization of Co extracted from the Co/Al_2O_3 interface in tunnel experiments is found to be *positive*, whereas the polarization of the full density of states at the Fermi energy is *negative*.

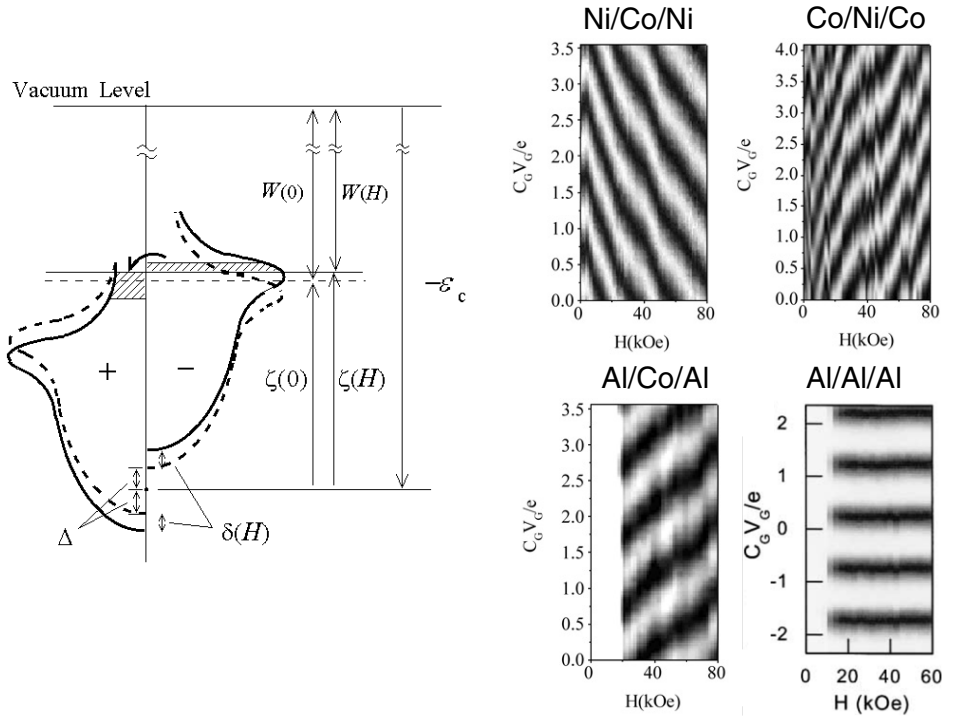

Figure 4. Left: diagram showing the repopulation and the field related Fermi energy ($\zeta(H)$) modified by the Zeeman splitting ($\delta(H)$). Right: grey-scale plots of $\mathrm{d}V/\mathrm{d}I$ versus V_g and H of Ni/Co/Ni, Co/Ni/Co, Al/Co/Al and Al/Al/Al SETs (see figure 3) with charging energies in the 50–100 μeV range. Darker regions indicate a higher conductance. The diagrams are taken at $V_{bias} = 0$ V and $T = 20$ mK. The vertical scale is converted to the number of gate induced electrons $C_g V_g/e$. Magneto-Coulomb induced conductance oscillations as a function of field are seen at a fixed gate voltage (horizontal cut) for the first three structures. As expected, the non-magnetic Al/Al/Al SET shows no oscillations. Adapted from [12, 14].

from the 'off' state ($Q_0 = 0$) to the 'on' state ($Q_0 = 0.5e$). A complete 'off' to 'off' cycle is obtained when $\Delta\mu = 2E_C = e^2/C_\Sigma$ (where $C_\Sigma = C_1 + C_2 + C_g$; see figures 3 and 5(A)) that is $\Delta Q_0 = e$. As the magnetic field is further swept, ΔQ_0 is increased, creating conductance oscillations while gradually passing through $1e/2, 3e/2 \ldots (2n+1)e/2$. These oscillations can be seen as a horizontal cut through the diagram of figure 4 and each time $\Delta Q_0 = e$ a cycle is run through. One can see in figure 4 that the fully non-magnetic Al/Al/Al SET shows no oscillations for the same cut. For intermediate applied fields H, we can rewrite the equivalent ΔQ_0 variation as

$$\Delta Q_0 = \frac{C_\Sigma}{e}\Delta\mu = \frac{C_\Sigma}{e}\frac{1}{2}P_{dot} g \mu_B \mu_0 H. \tag{6}$$

In a more general case, any component can be ferromagnetic. There, the variation of ΔQ_0 is induced either directly by acting on the ferromagnetic dot (weighted by the total dot's capacitance as seen above) or by a lever effect while acting on the ferromagnetic lead (weighted by the dot–lead capacitance). Here, one obtains

$$\Delta Q_0 = [C_\Sigma P_{dot} - (C_1 + C_2) P_{leads}] \frac{g\mu_B}{2e}\mu_0 H \tag{7}$$

where C_1 and C_2 are the capacitances as defined in figure 5 and $C_\Sigma = C_1 + C_2 + C_G$ is the total dot capacitance. The first term corresponds to the effect on the magnetic dot while the

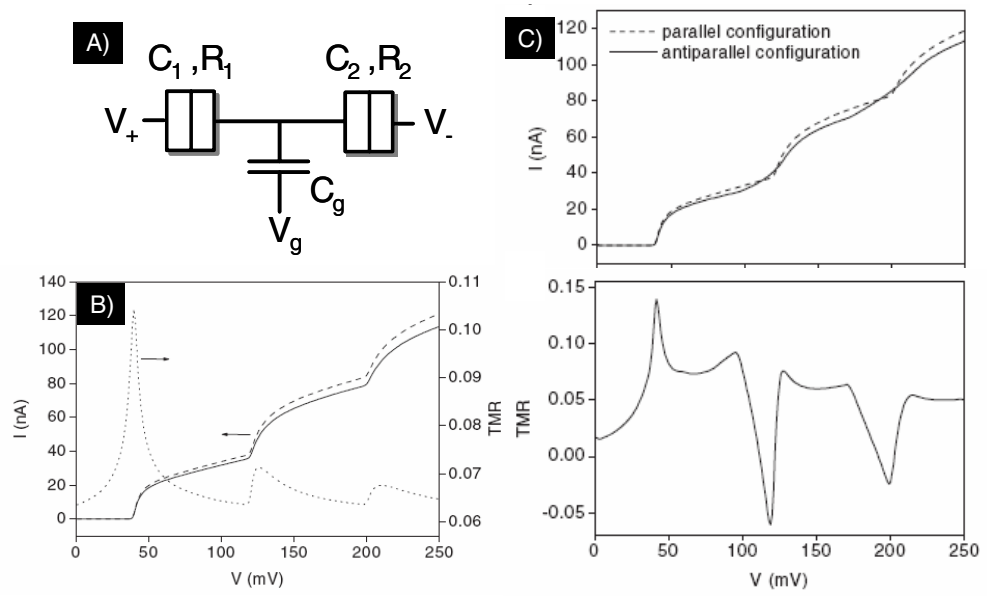

Figure 5. (A) Schematic diagram of a single electron transistor (SET), i.e. a dot connected to two electrodes via two tunnel junctions and linked to a gate via a capacitance. (B) $I(V)$ curve in the parallel (P) and antiparallel (AP) configurations of the magnetizations and TMR(V) expected for an F/F/F set in the absence of spin accumulation (short τ_{sf}). (C) $I(V)$ curves in the P and AP configuration and TMR(V) expected for an F/NM/F SET in the presence of spin accumulation (long τ_{sf}). For panels (B) and (C) [29], the parameters are $R^{P}_{1\uparrow} = 2R^{P}_{1\downarrow} = 5\,\mathrm{M\Omega}$, $R^{P}_{2\uparrow} = 2R^{P}_{2\downarrow} = 0.3\,\mathrm{M\Omega}$, $R^{P}_{i\uparrow} R^{P}_{i\downarrow} = R^{AP}_{i\uparrow} R^{AP}_{i\downarrow}$, $(i = 1, 2)$, $C_1 = C_2 = C_g = 1$ aF, $Q_0 = 0$, $V_g = 0$ and $T = 4.2$ K.

second term is related to the two electrodes (in this case considered to be made of the same material). Different combinations of ferromagnetic materials are presented in figure 4 with Ni/Co/Ni, Co/Ni/Co and Al/Co/Al SETs. The field induced shift can be upward or downward as it is weighted by the ferromagnet's polarization and the capacitance. This explains the inverse slopes for Ni/Co/Ni and Co/Ni/Co SETs seen in figure 4. In certain conditions dot and lead effects can compensate. It is also worth noting that only one ferromagnetic electrode is enough to induce an effect.

As a rule of thumb, oscillations can be observed as long as the maximum achievable Zeeman induced electrochemical potential shift is of the order of or higher than $2E_C = e^2/C_\Sigma$, $e^2/(C_1+C_2)$ or e^2/C_1 when respectively the dot, the two leads or the first lead is ferromagnetic. Taking into account laboratory achievable fields of the order of 16 T and P having an upper bound of 1, oscillations should only be observable for dots having charging energies below meV. Hence, a full magnetic field oscillation period cannot be seen in ultrasmall dots ($E_C \gg meV$) and at temperatures of liquid helium and above.

An interesting point we want to underline is that almost any nanostructure showing Coulomb blockade and having a ferromagnetic element could show significant magnetoresistance arising from this electrochemical potential shift (and therefore variation of Q_0). Depending on the configuration of the system, even $\Delta Q_0/e < 1\%$ (which is easily achievable for lead to dot capacitance of 100 aF and above) could induce MR effects much higher than 100%. Roughly speaking, in the case where very sharp Coulomb steps are expected (for high R_1 to R_2 ratio), if the applied voltage is close to the threshold one, a slight change in Q_0 may switch the system from the off to the on state (see figure 2). This shift will be

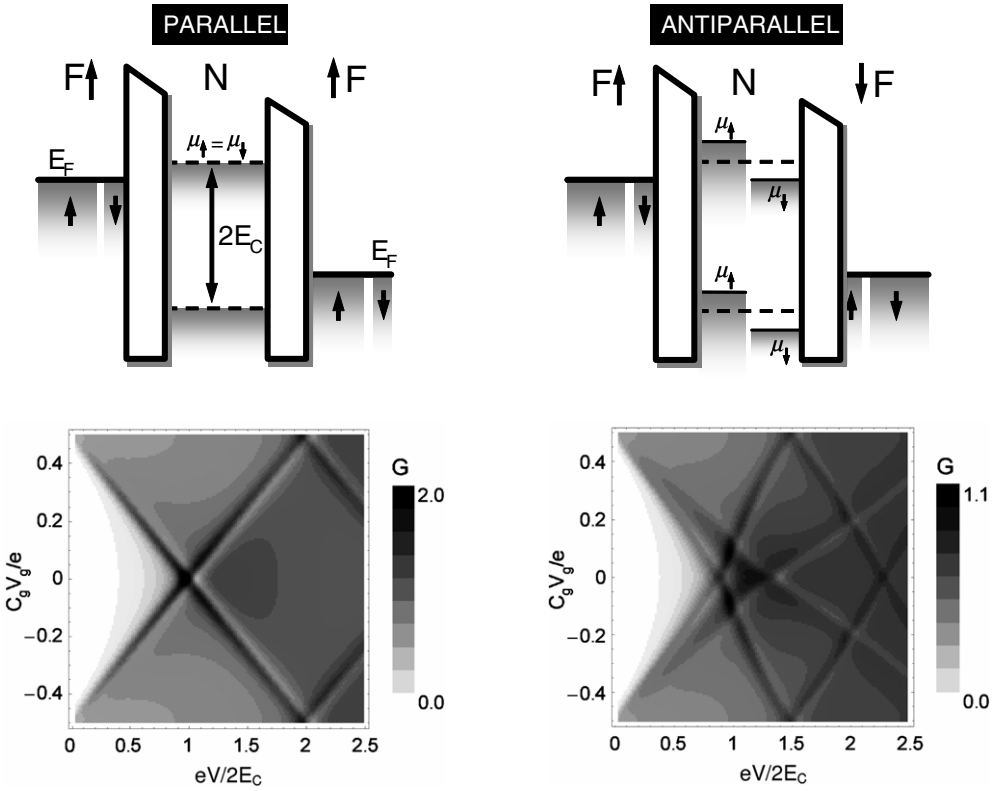

Figure 6. Simulations for an F/NM/F SET. Upper panel: energy diagram of an F/N/F SET in the parallel (left) and antiparallel (right) configurations of the magnetizations. Spin accumulation is shown in the AP case (long spin lifetime hypothesis). For the same applied voltage, the system is blocked in the P configuration and unblocked in the AP configuration due to the spin dependent electrochemical potential shift. The dashed line, which represents $(\mu_\uparrow + \mu_\downarrow)/2$, is at the same level in P and AP configurations. However, $\mu_\uparrow$ is at a lower level in the AP case. Lower panel: differential conductance G versus gate V_g and transport V voltages in a grey-scale representation in the P (left) and AP (right) configurations, calculated taking into account cotunnelling effects and showing spin accumulation effects in the AP case. The parameters are symmetric junctions with Fe electrodes (spin polarization $P = 0.4$), $T/E_C = 0.02$, $R^P_{1\uparrow} = R_{2\uparrow} = 5R_q$, $R^P_{1\downarrow} = R_{2\downarrow} = R_{2\uparrow}(1-P)/(1+P) = 0.43\ R_{2\uparrow}$ in the P case and $R^{AP}_{1\downarrow} = R_{2\uparrow}$, $R^{AP}_{1\uparrow} = R_{2\downarrow}$ in the AP case. The bottom diagrams are adapted from [40].

abrupt as the magnetization switches during a hysteresis cycle (the sign of P is reversed). Even single magnetic electrode (or dot) structures can give rise to magnetoresistance curves with a slope at zero field and only one clear switching field. A switching field of several hundred G could lead to a substantial effect for a dot having a charging of a few hundred μeV and below. Hence this effect should always be taken into account when analysing magnetoresistance data acquired on small nanostructures using ferromagnetic materials. Similar considerations were recently published [27, 28]. Finally, a similar effect could be expected in the case of single level quantum dots.

2.4. Interplay between spin and Coulomb blockade

Magnetoresistance oscillations versus applied voltage were the first magneto-Coulomb effect to be predicted. They were simultaneously predicted by [30] and [31]. The physical

origin of these oscillations is the step-like feature of Coulomb blockade combined with spin dependent tunnelling. Basically, as the step heights are controlled by the resistance of the junction, different step heights are expected in the parallel and antiparallel configuration of the magnetizations. This, combined with the non-linearity of the steps, would give rise to oscillations as a function of applied voltage in F/F/F, F/F/NM or NM/F/F double junctions as shown in figure 5(B). However, no effects were predicted for F/NM/F double junctions as spin accumulation was neglected. The effect of spin accumulation on the dot was introduced almost at the same time for F/F/NM [32] and F/NM/F double junctions in the sequential [33–35] and cotunnelling regimes [36]. The interesting feature was that spin accumulation could lead to a dynamic spin polarization at the Fermi level and hence to the occurrence of TMR and TMR oscillations even for the non-magnetic dot as seen in figure 5(C), contrary to the earlier model predictions. An interesting proposal was that of a ferromagnetic SET where the transport properties could be controlled either magnetically (by the configuration of the leads) or electrically (by the gate voltage). The behaviour of this SET was extensively analysed (see for example figure 6) in the sequential [29, 34, 37–39] and cotunnelling[2] regimes [40].

2.4.1. From spin accumulation to spin lifetime: principles. Let us consider the simplest case of an F/NM/F double junction in the 'orthodox' [41] situation with $\delta \ll kT \ll E_C$ (δ is the level spacing on the dot and E_C its charging energy) since energy level quantization is not crucial in the following. The structure is taken as symmetric (same tunnel barriers and ferromagnetic leads). As the electrodes are ferromagnetic, a spin polarized current is flowing into (and out of) the dot. In the parallel (P) configuration of the magnetizations, spin down (and spin up) electrons are injected and removed at the same rate from the unpolarized dot. The peaks due to Coulomb blockade are left unperturbed and appear at the same voltages that would be expected if the electrodes were non-magnetic (see figure 6, top left). On the other hand, in the anti-parallel (AP) configuration of the magnetizations, one spin direction (say up) is preferentially injected into the dot while the other (in this case down spin) is preferentially removed. If the spin lifetime τ_{sf} on the dot is long enough (as discussed below) an imbalance will appear giving rise to the spin accumulation effect: up spins will accumulate whereas down spins will deplete. As this phenomenon appears (see figure 6, top right), the Fermi energy on the cluster splits into up spin ($\mu_\uparrow$) and down spin ($\mu_\downarrow$) electrochemical potentials affecting the Coulomb thresholds. Here, the splitting is considered to be uniform over the dot, which, in the diffusive limit, is true if the dot is smaller than the usual GMR spin diffusion length defined for non-magnetic metals: $l_{sf} = \sqrt{D\tau_{sf}}$, where D is the electron diffusion constant in the dot [42]. The number of accumulated spins N_s (and hence the magnetization of the dot) can be related to the resulting out of equilibrium $\Delta\mu = \mu_\uparrow - \mu_\downarrow$ through the formula $\Delta\mu = N_s\delta$. In a simplified view, as the spin accumulation sets in, the depleted down spins have their electrochemical potential shifted downward (just as a ΔQ_0 would do), reducing the threshold voltage for the onset of the down spin single electron current. Close to the original threshold voltage, this gives rise to a higher current in the antiparallel case where spin accumulation occurs, hence giving an inverse TMR [32, 34, 35] (see figure 5(C)). It is worth noting that spin accumulation due to the cotunnelling current can already be present in the Coulomb gap, leading to the above effects even on the first peak [36]. As an example, SET diagrams taking into account the cotunnelling effect and highlighting the peak splitting due to spin accumulation in the antiparallel configuration are shown at the bottom of figure 6. Interestingly, the spin accumulation can be directly probed by the Coulomb peak splitting [43].

[2] Around the Coulomb thresholds, the cotunnelling and sequential tunnelling terms are potentially of the same order of magnitude.

A way to confirm the origin of the effect is to apply a field perpendicularly to the magnetizations of the leads, inducing a Larmor precession of the injected spins (Hanle effect) and therefore reducing the spin accumulation [44–46].

Let us now express the conditions leading to the appearance of spin accumulation. In order to simplify the explanation, in the following, we assume again that the structure is symmetric (same tunnel barriers and ferromagnetic leads). As an order of magnitude estimation, one can consider that for an injected electron on the dot the time for which its spin is conserved (spin lifetime) must be longer than the time spent on the dot (dwell time). Therefore, one can write $\tau_{sf} > \tau_{dwell} \sim e/I$, where I is the single electron current flowing through the system. More precisely, the order of magnitude condition can be reformulated in a steady current regime as the number of spins relaxing per unit time being equal to those injected on the dot

$$N_s/\tau_{sf} = PI/e \sim \Delta\mu/(\delta\tau_{sf}) = PV/eR, \tag{8}$$

where V is the applied bias, R the lead/dot resistance and P the spin polarization of the electrode. As expressed by [33], one can consider that the spin accumulation significantly affects the transport properties when $\Delta\mu \geqslant eV$. Then the condition on the appearance can be rewritten as

$$\delta\tau_{sf}/h > R/R_q \gg 1 \tag{9}$$

where $R_q = h/e^2$ and $R/R_q \gg 1$ has been chosen in order to fulfil the Coulomb blockade condition. This highlights the required conditions of large level spacing δ and/or long spin lifetime τ_{sf} associated with low tunnel resistance for spin accumulation to occur. One could expect this in very small dots, where the level spacing is intrinsically increased as the dot's dimensions are reduced, and/or in dots made of light elements with small spin–orbit coupling.

We now try to extract quantitative information on the spin lifetime in the same F/NM/F double junction. In the antiparallel configuration one can balance the spin currents through the cluster by writing that the up spin current going through the second junction $I_{2\uparrow}$ is equal to the one going through the first junction $I_{1\uparrow}$ plus spins flipping from down to up, minus spins flipping from up to down:

$$I_{2\uparrow} = I_{1\uparrow} + \frac{eN_\downarrow(E_F)\mu_\downarrow}{\tau_{sf}} - \frac{eN_\uparrow(E_F)\mu_\uparrow}{\tau_{sf}} \tag{10}$$

where $N_{\uparrow(\downarrow)}(E_F)$ is the density of states at the Fermi energy for up spins (down spins)[3]. For low enough voltages, which correspond to the lowest order perturbation from the spin accumulation, the junctions can be considered fully symmetric and one can write $I_{2\uparrow} = I_{1\downarrow}$, giving $I_{1\uparrow(\downarrow)} = (1 \pm P_{Co})I/2$. Finally, equation (10) can be rewritten

$$\tau_{sf} = \frac{eN(E_F)\Delta\mu}{2PI}, \tag{11}$$

where τ_{sf} is simply expressed as a function of the spin accumulation on the dot $\Delta\mu$. One can then straightforwardly obtain the value of τ_{sf} on the dot by measuring the spin accumulation induced Coulomb peak splitting between the parallel and antiparallel case. This can be a way to directly probe the spin lifetime in a nanometre sized nano-object, where four probe measurements are nearly impossible [42, 47], without relying on indirect measurements [46, 48, 49].

[3] For non-magnetic noble metals such as Au or Cu, $N_\downarrow(E) = N_\uparrow(E) = N(E)/2$ can be assumed to be constant over the range of the electrochemical potential split $E = E_F \pm \Delta\mu/2$ in the limit of small spin accumulation.

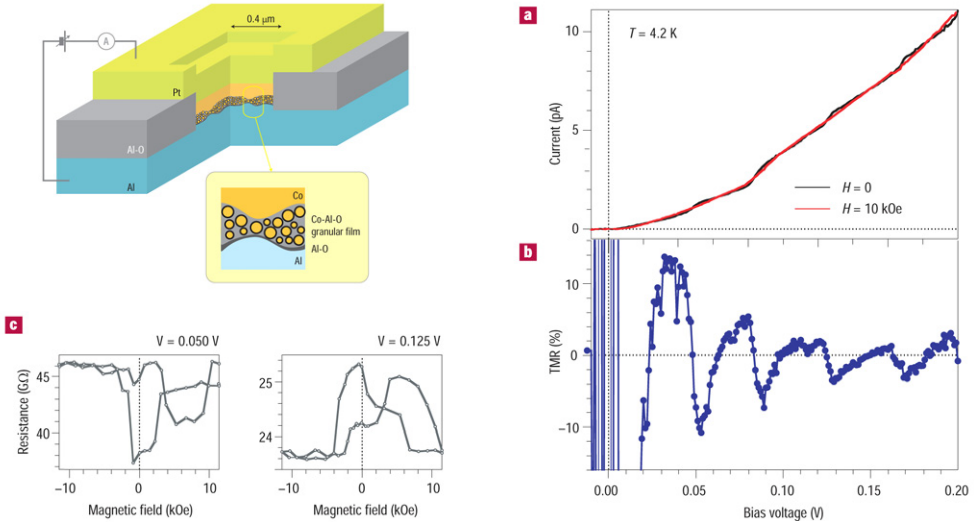

Figure 7. Top left: schematic illustration of a sample with a pillar structure. The structure is a Al/Al–O/Co–Al–O granular film (15 nm)/Co/Pt multilayer microfabricated by electron-beam lithography and Ar-ion milling process to reduce the contact area to $0.4 \times 0.4\ \mu m^2$. Although the nominal thickness of the Co–Al–O is 15 nm, which corresponds to that of three or four particles, the authors estimate that the current-dominating path has only one or at most two particles in that layer because of its roughness. Magnetotransport properties at $T = 4.2$ K. (a) $I(V)$ curves at $H = 0$ and $H = 10$ kOe, (b) TMR(V) showing oscillations as a function of bias voltage and (c) TMR at $V = 0.05$ and $V = 0.12$ V. Adapted from [49].

2.4.2. From spin accumulation to spin lifetime: experiments. We now focus on the experimental results. The oscillatory behaviour of the TMR was first seen in granular CoAlO nanobridges having an in-plane (CIP) geometry and containing a relatively large number of clusters of 2.5 nm average diameter in series and parallel [50]. A different vertical geometry (CPP) was developed (see figure 7) containing fewer clusters in series while more in parallel [49, 51]. Enhanced TMR above the threshold voltage was found in both cases. While the oscillations were strongly damped in the in-plane case, several periods could be seen in the vertical one. Since then, both in plane [52] and vertical structures have been optimized [53], showing clearer effects. For the vertical structure (see figure 7, left), although the authors acknowledge the possibility of over 10^4 current paths in parallel and up to three or four particles in series in the 15 nm thick Co–Al–O, they estimate that the current-dominating path has only one or at most two particles in that layer because of its roughness [49]. Hence, while qualitatively agreeing, these results are difficult to relate to the single dot theory as the number of clusters involved in the transport process remains unknown. It has been shown theoretically that several clusters in series could still lead to the observation of a Coulomb staircase [54] and TMR oscillations [55].

A way to partly circumvent the aforementioned problem is the use of tunnel junctions including a single 2D array of clusters as first done by Schelp *et al* [9]. Encouraging results were also obtained in epitaxially grown Fe/MgO/Fe/MgO/Co double junctions with pancake-like Fe clusters of 3.4 nm average diameter [56]. Although one would have expected the effect to be either smeared or averaged out, positive TMR oscillations similar to the ones predicted by the first theories were clearly observed.

Connecting a *single* nanometre sized object with non-magnetic leads is already a challenge. Hence, few experimental papers on the transport spectroscopy of single nanometre sized dots

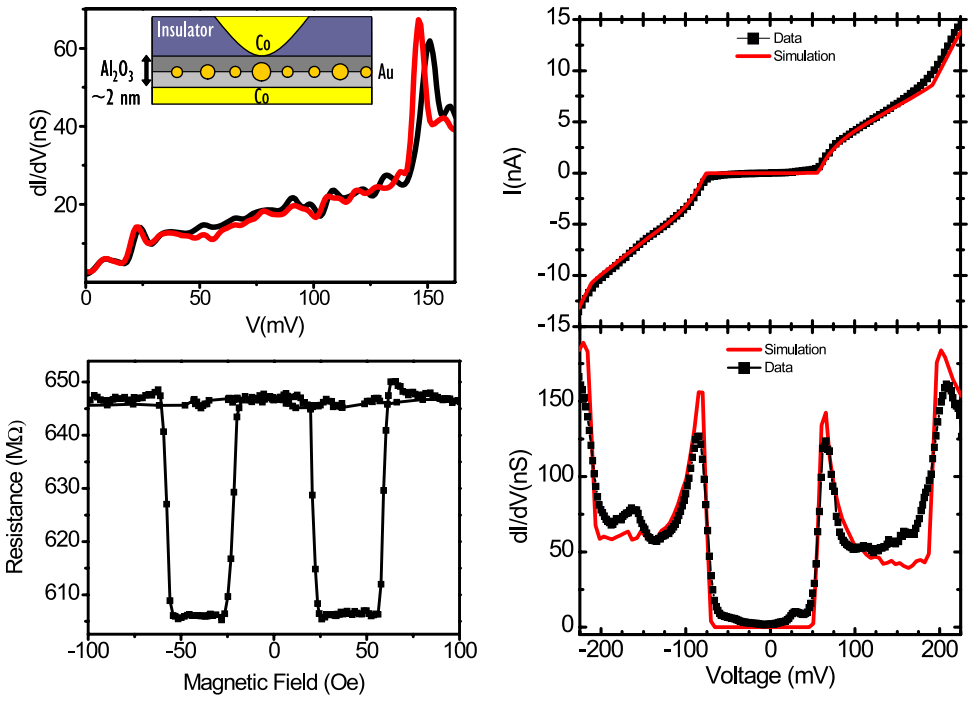

Figure 8. Inset of the top left figure: schematic cross-section of the patterned structure showing the top/bottom Co electrodes and the 2D assembly of nanoparticles embedded in a thin alumina layer. The effective nanocontact cross section is less than 10 nm and a single nanoparticle is connected. Top left: $\mathrm{d}I/\mathrm{d}V(V)$ curve for a single Au cluster of ∼3 nm in the parallel (black) and antiparallel (red) magnetic configurations of the Co electrodes [67]. Note the peak shifting (larger on the second peak) in the antiparallel configuration. The shape of the curve corresponds to the high value of $Q_0 = 0.4e$ (see [66]). Right: black line and ■, $I(V)$ curve at 4.2 K on another sample of 2.5 nm (top) and $\mathrm{d}I/\mathrm{d}V(V)$ curve (bottom) obtained by differentiating the above $I(V)$. Red line, single particle simulation using the parameters $C_1 = 0.4$ aF, $C_2 = 1.14$ aF, $R_2 = 3R_1$ and $Q_0 = 0.07e$. Bottom left: resistance versus magnetic field of the same sample obtained at 20 mV and 4.2 K. Adapted from [66].

in a magnetic field have been published [48, 57, 58], with only two dealing with a cobalt nanoparticle [59, 60][4]. However, the enhanced technological difficulty that represents the connection of two ferromagnetic leads via two tunnel junctions to a single nanometre sized object certainly explains why hardly any early experimental results have been reported until now. Only two groups have already reported their ability to take up this challenge. The preliminary results were for a Co/Co/Au double junction [62] showing no magnetic effects and a Ni/Al/Al double junction [63]. They were followed by a Ni/C_{60}/Ni SET showing the Kondo effect [64] (see section 3.1.3). Very recently, evidence for the connection of a single gold cluster of 2.5 nm in diameter linked to two cobalt leads was demonstrated. The structure, schematically shown in the inset in the top left part of figure 8, was obtained using a nanoindentation technique relying on a conductive tip AFM [65]. This technique enables the fabrication of a nanocontact with a cross section of less than 10 nm. The $I(V)$ and $\mathrm{d}I/\mathrm{d}V(V)$, associated with a single cluster simulation at $Q_0 = 0.07e$, clearly showing that the transport process occurs though a single cluster, are presented on the right of figure 8. In addition, an inverse TMR related to the

[4] For a recent review on the spectroscopy of energy levels in nanoparticles, the reader should refer to [61].

spin transport through the non-magnetic nanoparticle was observed [66] (see figure 8, bottom left). As illustrated in figure 8 and following equation (11), the analysis of the spin transport in the framework of the spin accumulation for another single Au nanoparticle leads to a spin lifetime of 800 ps [67]. This spin lifetime is significantly enhanced when compared to quench condensed thin films or wires [68, 69].

3. Future directions

3.1. Quantum dots

Here, we will briefly focus onto the problem of dots connected to ferromagnetic leads and do not treat the wide topic of spin injection/manipulation using magnetic fields in mesoscopic semiconductor quantum dots[5]. As the dot size is reduced, its energy spectrum changes from continuous to discrete (δ being inversely proportional to the volume of the dot) and additional features in the transport properties are expected [72, 73]. For metallic dots, temperatures well below liquid helium temperature are required as nanoparticles below 10 nm have level spacing around meV. The extreme case corresponds to a semiconductor quantum dot with a single level. In the following we will consider the limit $k_{\mathrm{B}}T, eV \ll \delta$.

3.1.1. Quantum dots weakly coupled to ferromagnetic leads. We now concentrate on the weak coupling regime. Effects such as spin blockade, diode-like features or negative differential conductance were predicted. This was studied for collinear configurations of the magnetization [74] in the sequential regime [75, 76] and cotunnelling regime [77, 78]. Spin flip on the dot [79, 80], noise correlation [75, 81–83] and spin torque [84] were also studied. Extension was made to the case of arbitrary noncollinear magnetizations of the electrodes, where a precession of the dot's spin around an effective exchange field in the dot gives rise to non-trivial angular dependence [85–92].

As seen above, there has been an intense activity during recent years on the theoretical side as one could think of manipulating and probing single spins in quantum dots. However, as far as experiments are concerned, the technological challenge that represents such structure explains the lack of results. Only very few results with no specific connection to the above theory have been obtained in the quest to contact a quantum dot to ferromagnetic leads in the weak coupling regime. The first result was obtained on an aluminium dot connected to a single ferromagnetic nickel or cobalt lead, probing single levels at very low temperatures [63]. The conjugated effect of using a ferromagnetic lead and Zeeman splitting was used to evaluate the spin dependent tunnelling rates and the spin polarization of the ferromagnet. Very recently, Wunderlich *et al* [93] created a single electron transistor with p-type (Ga, Mn)As showing a large magnetoresistance that could be reverted using the gate voltage (see figure 9(A)). However, the effects were interpreted as due to the electrochemical potential shift induced by the magnetization rotation in this strongly spin–orbit coupled system in a way similar to the one presented in section 2.3.

3.1.2. Carbon nanotubes coupled to ferromagnetic leads. While not going into detail, we just quickly introduce carbon nanotubes as they are certainly one of the most interesting ways towards quantum dots. Single electron and/or quantum interference effects can already be observed in these ballistic 1D systems. By tuning the contact coupling to the nanotube, one can range from a quasi-quantum dot or 1D quantum well [96] showing Coulomb blockade and shell filling [97–100] (weak coupling or low transparency contact) to a quantum

[5] For recent reviews, the reader should refer to [70, 71].

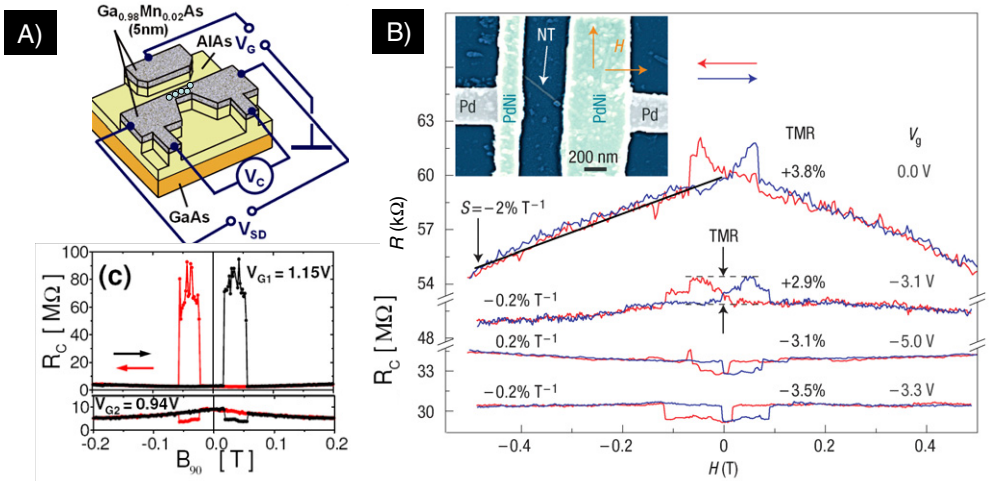

Figure 9. (A) Top, schematic representation of the gated $Ga_{0.98}Mn_{0.02}As$ magnetic semiconductor transistor. The blue dots represent the possible dots. From [94]. Bottom, magnetoresistance curve at $T = 4.2$ K showing a change in sign for different gate voltages V_G. Adapted from [93]. (B) Inset: SEM picture of a carbon nanotube contacted with PdNi electrodes. The separation between the electrodes along the nanotube is 400 nm. Main panel: magnetoresistance curve at $T = 1.85$ K for different gate values V_G. The TMR sign reverses as a function of gate voltage. Adapted from [95].

interferometer [96, 101] such as a Fabry–Perot resonator [102] (strong coupling or high transparency contact). Moreover, their commercial availability and their long length of several hundred nanometres have made them a primary choice to elaborate gated nanostructures without requiring preliminary knowledge of cutting edge lithography techniques. Hence, they have undergone several successful studies in the past years. From the spin dependent transport point of view, negligible spin orbit coupling correlated to high Fermi velocities make them very good candidates (more viable than most of the low Fermi velocity semiconductors) for long distance lateral spin transport. Early work on ferromagnetic electrodes connected to nanotubes started with the evidence for a 250 nm spin coherence length in a multiwall carbon nanotube (MWNT) with Co electrodes [103]. An interesting fact is that a positive magnetoresistance of 9% [103] and a high negative magnetoresistance of −30% were found for similar systems [104] with Co electrodes. We present results for NiPd contacts on a gated 400 nm long MWNT in figure 9(B). In the past few years, focus has been put on the simpler single wall nanotubes (SWNTs) [28, 105, 106]. In these systems, gate controlled sign changes of the magnetoresistance were observed [95, 107–109]. Whereas the effects are still not fully understood, an interpretation based on quantum interference and the near resonance Breit–Wigner formula was proposed [95]. In the coming years, carbon nanotubes will certainly prove to be one of the most unique and accessible ways of probing the interplay between spin, single electron and quantum effects. This may happen thanks to the mastering of reliable high or low transparency ferromagnetic contacts (for example high transparency contacts made of Pd alloys [95] initially developed to reduce the Schottky barrier [110] can be used) conjugated to the increasing quality of the SWNT.

3.1.3. The Kondo effect. In the case of strong coupling between the dot and the leads, a Kondo effect may be expected. The many body Kondo effect was predicted in quantum dots

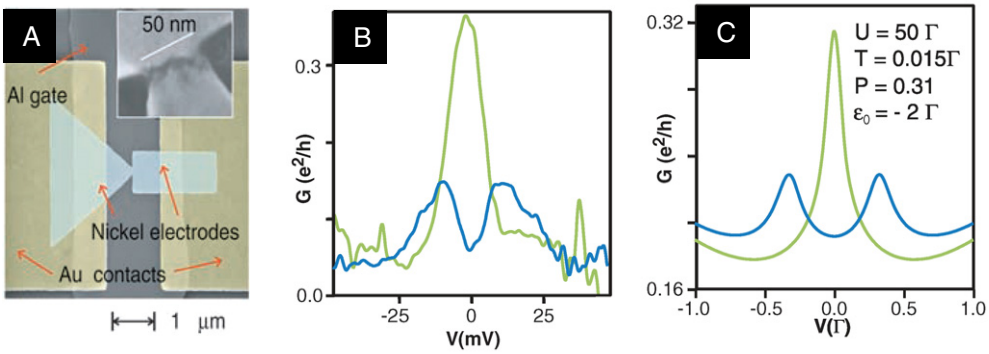

Figure 10. (A) Scanning electron micrograph of a Ni break junction. The magnetic field is applied in the horizontal direction. Inset, close-up of the junction region after electromigration. (B) Conductance curves for Ni–C_{60}–Ni devices at $T = 1.5$ K: blue, magnetizations parallel, $B = 250$ mT; green, magnetizations approximately antiparallel, $B = 15$ mT. (C) Theoretical fit of panel (B) using reference [116]. The figure is adapted from reference [64].

attached to non-magnetic leads almost two decades ago [111, 112][6]. If the electron number is odd on the quantum dot, the topmost level is singly occupied. When the temperature is low enough (below the Kondo temperature), a Kondo resonance arises from the antiferromagnetic coupling between the spin of the localized electron on the dot and the conduction band electrons of the leads. This leads to a peak in the conductance at zero bias (see figures 10(B), (C), green curve). However, the main condition for this to occur is the spin degeneracy of the dot's level. The effect of replacing the non-magnetic electrodes with ferromagnetic ones has been actively studied very recently [114–123] with further extensions to the three terminal [124], gated [125] or double quantum dot [126, 127] case. On the experimental side, only one result was reported, where a gated single C_{60} molecule was linked to Ni electrodes [64] as shown in figue 10(A). To summarize the results, the Kondo anomaly becomes partially or totally suppressed in the parallel magnetization configuration (see figures 10(B), (C), blue curve) while features similar to the non-magnetic situation are present in the antiparallel configuration for symmetric junctions (see figures 10(B), (C), green curve). The suppression of the Kondo anomaly arises as a consequence of the effective exchange field induced by the interaction with the ferromagnetic leads. The Kondo resonance splits into two peaks moving away from the Fermi level, hence suppressing the conductance anomaly in a way equivalent to an applied magnetic field. The anomaly can then be restored by applying the right compensating magnetic field as confirmed experimentally in a gated single C_{60} molecule linked to Ni electrodes [64] (see figure 10).

3.2. Nanomagnets and single molecule magnets

Ferromagnetic nanoparticles of a few nanometres in diameter (nanomagnets) can become smaller than the exchange length and reasonably be considered as single domains (for example 7 nm in cobalt [128]). They can hence be played with as model systems for the study of the interaction of transport and magnetism. Transport characteristics of a single cobalt nanomagnet coupled to non-magnetic leads have been studied using single electron spectroscopy both experimentally [59, 60] and theoretically [129–131]. Experimentally, a denser than expected spectrum of tunnelling excitations was found and discrete energy level shifts were associated

[6] For a review on the Kondo effect in quantum dots the reader could refer to [113].

with the magnetic moment reorientation. Further recent theories have predicted the dynamics of nanomagnets, including the behaviour of spin torque, magnetization reversal and stabilized precessional states [132–136].

With the advent of molecular spintronics [137, 138], an emerging field is the study of transport through single molecule magnets (SMMs) such as Mn_{12} or Fe_8 showing a large spin S. Weak intermolecular interactions have helped the study of the magnetization and anisotropy barrier and quantum tunnelling in thin films and bulk SMM crystals [139–141]. As an example, steps observed in the hysteresis cycle have been attributed to quantum tunnelling between degenerate states of the magnetization. Mn_{12} acetate, with a total spin $S = 10$, has been the main subject of these extensive studies. As far as transport is concerned, very few theoretical studies have been performed [142, 143] and it is only very recently that a single Mn_{12} was trapped in a nanogap between non-magnetic electrodes [144]. Spin blockade and negative differential conductance explained by transport in the sequential regime were observed. However, no experiments with at least one single ferromagnet connected to an SMM have been reported so far. This would be very interesting, as spin injection could shed new light on probing the quantum magnetic properties of the SMM.

4. Conclusion

On the way towards the transport and manipulation of spins in nanometre sized nanostructures connected to ferromagnetic electrodes some steps have been carried out. Effects combining single electron and spin properties such as TMR enhancement, spin accumulation or magneto-Coulomb shifts have been observed in mesoscopic structures or in nanoparticle assemblies. However, results on a single nanometre sized object connected to at least one ferromagnetic reservoir have scarcely appeared, leaving the field wide open for future experiments. Here, it is clear that the underlying technological challenge has made the experimental progress much slower than the theoretical one. In this respect, molecular nanospintronics, which adds the degrees of freedom of molecular engineering to nanoscale spintronics, is a promising route.

Several steps remain to be undertaken on the path to spin transport and manipulation at the nanoscale. The future will decide whether or not the different approaches presented in this review will succeed in generating novel nanospintronic devices or demonstrating coherent spin control leaning towards qubits and quantum computation.

Acknowledgments

The authors wish to deeply thank R Mattana and A Anane for their thoughtful comments and insights on the manuscript.

References

[1] Averin D V and Nazarov Y V 1990 Virtual electron diffusion during quantum tunneling of the electric charge *Phys. Rev. Lett.* **65** 2446

[2] Likharev K K 1988 Correlated discrete transfert of single electron in ultrasmall tunnel junctions *IBM J. Res. Dev.* **32** 144

[3] Likharev K K 1999 Single-electron devices and their applications *Proc. IEEE* **87** 606

[4] Grabert M H and Devoret M (ed) 1992 *Single Charge Tunneling, Coulomb Blockade Phenomena in Nanostructures* (*NATO Advanced Study Institute, Series B: Physics* vol 294) (New York: Plenum)

[5] Hanna A E and Tinkham M 1991 Variation of the Coulomb staircase in a tow-junction system by fractional electron charge *Phys. Rev.* B **44** 5919

[6] Gittleman J I, Goldstein Y and Bozowski S 1972 Magnetic properties of granular nickel films *Phys. Rev.* B **5** 3609
[7] Helman J S and Abeles B 1976 Tunneling of spin-polarized electrons and magnetoresistance in granular Ni films *Phys. Rev. Lett.* **37** 1429
[8] Fujimori H, Mitani S and Ohnuma S 1995 Tunnel-type GMR in metal-nonmetal granular alloy thin films *Mater. Sci. Eng.* B **31** 219
[9] Schelp L F, Fert A, Fettar F, Holody P, Lee S F, Maurice J L, Petroff F and Vaures A 1997 Spin-dependent tunneling with Coulomb blockade *Phys. Rev.* B **56** R5747
[10] Dieny B, Sankar S, McCartney M R, Smith D J, Bayle-Guillemaud P and Berkowitz A E 1998 Spin-dependent tunneling in discontinuous metal/insulator multilayers *J. Magn. Magn. Mater.* **185** 283
[11] Ono K, Shimada H, Kobayashi S and Ootuka Y 1996 Magnetoresistance of ni/nio/co small tunnel junctions in Coulomb blockade regime *J. Phys. Soc. Japan* **65** 3449
[12] Shimada H, Ono K and Ootuka Y 1998 Magneto-Coulomb oscillation in ferromagnetic single electron transistor *J. Phys. Soc. Japan* **67** 1359
[13] Ono K, Shimada H and Ootuka Y 1998 Ferromagnetic single electron transistor *Solid-State Electron.* **42** 1407
[14] Ootuka Y, Ono K, Shimada H, Matsuda R and Kanda A 2001 Electron transport in ferromagnetic small tunnel junctions *Mater. Sci. Eng.* B **84** 114
[15] Ono K, Shimada H and Ootuka Y 1997 Enhanced magnetic valve effect and magneto-Coulomb oscillations in ferromagnetic single electron transistor *J. Phys. Soc. Japan* **66** 1261
[16] Mitani S, Takanashi K, Yakushiji K and Fujimori H 1998 Anomalous behavior of temperature and bias-voltage dependence of tunnel-type giant magnetoresistance in insulating granular systems *J. Appl. Phys.* **83** 6524
[17] Bruckl H, Reiss G, Vinzelberg H, Bertram M, Monch I and Schumann J 1998 Enhanced magnetoresistance of permalloy/Al-oxide/cobalt tunnel junctions in the Coulomb blockade regime *Phys. Rev.* B **58** R8893
[18] Zhu T and Wang Y J 1999 Enhanced tunneling magnetoresistance of Fe–Al2O3 granular films in the Coulomb blockade regime *Phys. Rev.* B **60** 11918
[19] Takahashi S and Maekawa S 1999 Enhancement in spin-dependent tunneling with Coulomb blockade *J. Magn. Magn. Mater.* **198** 143
[20] Iwabuchi S, Tanamoto T and Kitawaki R 1998 Coulomb blockade and enhancement of magnetoresistance change in ultrasmall ferromagnetic tunnel junctions *Physica* B **249** 276
[21] Takahashi S and Maekawa S 1998 Effect of Coulomb blockade on magnetoresistance in ferromagnetic tunnel junctions *Phys. Rev. Lett.* **80** 1758
[22] Guinea F 1998 Spin-flip scattering in magnetic junctions *Phys. Rev.* B **58** 9212
[23] Sukegawa H, Nakamura S, Hirohata A, Tezuka N and Inomata K 2005 Significant magnetoresistance enhancement due to a cotunneling process in a double tunnel junction with single discontinuous ferromagnetic layer insertion *Phys. Rev. Lett.* **94** 068304
[24] Wang X H and Brataas A 1999 Large magnetoresistance ratio in ferromagnetic single-electron transistors in the strong tunneling regime *Phys. Rev. Lett.* **83** 5138
[25] Ootuka Y, Matsuda R, Ono K and Shimada H 2000 Spin polarization and magneto-Coulomb oscillations in ferromagnetic single-electron transistors *Physica* B **280** 394
[26] Shimada H, Ono K and Ootuka Y 2003 Driving the single-electron device with a magnetic field *J. Appl. Phys.* **93** 8259
[27] vander Molen S J, Tombros N and van Wees B J 2006 Magneto-Coulomb effect in spin-valve devices *Phys. Rev.* B **73** 220406
[28] Tombros N, van der Molen S J and van Wees B J 2006 Separating spin and charge transport in single-wall carbon nanotubes *Phys. Rev.* B **73** 233403
[29] Weymann I and Barnas J 2003 Transport characteristics of ferromagnetic single-electron transistor *Phys. Status Solidi* b **236** 651
[30] Barnas J and Fert A 1998 Magnetoresistance oscillations due to charging effects in double ferromagnetic tunnel junctions *Phys. Rev. Lett.* **80** 1058
[31] Majumdar K and Hershfield S 1998 Magnetoresistance of the double-tunnel-junction Coulomb blockade with magnetic metals *Phys. Rev.* B **57** 11521
[32] Barnas J and Fert A 1998 Effects of spin accumulation on single electron tunneling in a double ferromagnetic microjunction *Europhys. Lett.* **44** 85
[33] Brataas A, Nazarov Y V, Inoue J and Bauer G E W 1999 Spin accumulation in small ferromagnetic double-barrier junction *Phys. Rev.* B **59** 93
[34] Korotkov A N and Safarov V I 1999 Nonequilibrium spin distribution in a single-electron transistor *Phys. Rev.* B **59** 89

[35] Barnas J and Fert A 1999 Interplay of spin accumulation and Coulomb blockade in double ferromagnetic junctions *J. Magn. Magn. Mater.* **192** 391
[36] Imamura H, Takahashi S and Maekawa S 1999 Spin-dependent Coulomb blockade in ferromagnet/normal-metal/ferromagnet double tunnel junctions *Phys. Rev.* B **59** 6017
[37] Kuo W and Chen C D 2002 Gate-controlled spin polarized current in ferromagnetic single electron transistors *Phys. Rev.* B **65** 104427
[38] Brataas A and Wang X H 2001 Linear response conductance and magnetoresistance of ferromagnetic single-electron transistors *Phys. Rev.* B **64** 104434
[39] Wetzels W, Bauer G E W and Grifoni M 2005 Noncollinear single-electron spin-valve transistors *Phys. Rev.* B **72** 020407
[40] Martinek J, Barnas J, Maekawa S, Schoeller H and Schon G 2002 Spin accumulation in ferromagnetic single electron transistors in the cotunneling regime *Phys. Rev.* B **66** 014402
[41] Likharev K K 1987 Single-electron transistors: electrostatic analogs of the DC SQUIDS *IEEE Trans. Magn.* **23** 1142
[42] Zaffalon M and van Wees B J 2003 Zero-dimensional spin accumulation and spin dynamics in a mesoscopic metal island *Phys. Rev. Lett.* **91** 168601
[43] Martinek J, Barnas J, Maekawa S, Schoeller H and Schon G 2002 Spin accumulation and cotunneling effects in ferromagnetic single-electron transistors *J. Magn. Magn. Mater.* **240** 143
[44] Hernando H D, Nazarov Y V, Brataas A and Bauer G E W 2000 Conductance modulation by spin precession in noncollinear ferromagnet normal-metal ferromagnet systems *Phys. Rev.* B **62** 5700
[45] Braun M, Konig J and Martinek J 2005 Hanle effect in transport through quantum dots coupled to ferromagnetic leads *Europhys. Lett.* **72** 294
[46] Zhang L Y, Wang C Y, Wei Y G, Liu X Y and Davidovic D 2005 Spin-polarized electron transport through nanometer-scale al grains *Phys. Rev.* B **72** 155445
[47] Filip A T, Jedema F J and van Wees B J 2001 Electrical spin injection and accumulation at room temperature in an all-metal mesoscopic spin valve *Nature* **410** 345
[48] Petta J R and Ralph D C 2001 Studies of spin–orbit scattering in noble-metal nanoparticles using energy-level tunneling spectroscopy *Phys. Rev. Lett.* **87** 266801
[49] Yakushiji K, Ernult F, Imamura H, Yamane K, Mitani S, Takanashi K, Takahashi S, Maekawa S and Fujimori H 2005 Enhanced spin accumulation and novel magnetotransport in nanoparticles *Nat. Mater.* **4** 57
[50] Mitani S, Takanashi K, Yakushiji K, Chiba J and Fujimori H 2001 Study on spin dependent tunneling and Coulomb blockade in granular systems with restricted tunneling paths *Mater. Sci. Eng.* **84** 120
[51] Yakushiji K, Mitani S and Takanashi K 2002 Tunnel magnetoresistance oscillations in current perpendicular to plane geometry of coalo granular thin films *J. Appl. Phys.* **91** 7038
[52] Yakushiji K, Matsuura M, Mitani S, Takanashi K and Fujimori H 2006 Coulomb staircase and tunnel magnetoresistance in nanowire shaped granular films *J. Magn. Magn. Mater.* **303** e355
[53] Yamane K, Yakushiji K, Ernult F, Matsuura M, Mitani S, Takanashi K and Fujimori H 2004 Inverse tunnel magnetoresistance associated with Coulomb staircases in micro-fabricated granular systems *J. Magn. Magn. Mater.* **272–276** e1091
[54] Imamura H, Chiba J, Mitani S, Takanashi K, Takahashi S, Maekawa S and Fujimori H 2000 Coulomb staircase in STM current through granular films *Phys. Rev.* B **61** 46
[55] Weymann I and Barnas J 2006 Negative differential conductance and magnetoresistance oscillations due to spin accumulation in ferromagnetic double-island devices *Phys. Rev.* B **73** 033409
[56] Ernult F, Yamane K, Mitani S, Yakushiji K, Takanishi K, Takahashi Y K and Hono K 2004 Spin-dependent single-electron-tunneling effects in epitaxial Fe nanoparticles *Appl. Phys. Lett.* **84** 3106
[57] Ralph D C, Black C T and Tinkham M 1995 Spectroscopic measurements of discrete electronic states in single metal particles *Phys. Rev. Lett.* **74** 3241
[58] Davidović D and Tinkham M 1999 Spectroscopy, interactions, and level splittings in Au nanoparticles *Phys. Rev. Lett.* **83** 1644
[59] Gueron S, Deshmukh M M, Myers E B and Ralph D C 1999 Tunneling via individual electronic states in ferromagnetic nanoparticles *Phys. Rev. Lett.* **83** 4148
[60] Deshmukh M M, Kleff S, Guéron S, Bonet E, Pasupathy A N, von Delft J and Ralph D C 2001 Magnetic anisotropy variations and nonequilibrium tunneling in a cobalt nanoparticle *Phys. Rev. Lett.* **87** 226801
[61] Von Delft J and Ralph D C 2001 Spectroscopy of discrete energy levels in ultrasmall metalic grain *Phys. Rep.* **345** 61
[62] Desmicht R, Faini G C, Cros V, Fert A, Petroff F and Vaures A 1998 Point-contact electrodes to probe charging effects in individual ultrasmall cobalt clusters *Appl. Phys. Lett.* **72** 387

[63] Deshmukh M M and Ralph D C 2002 Using single quantum states as spin filters to study spin polarization in ferromagnets *Phys. Rev. Lett.* **89** 266803
[64] Pasupathy A N, Bialczak R C, Martinek J, Grose J E, Donev L A K, McEuen P L and Ralph D C 2004 The Kondo effect in the presence of ferromagnetism *Science* **306** 86
[65] Bouzehouane K, Fusil S, Bibes M, Carrey J, Blon T, Le Du M, Seneor P, Cros V and Vila L 2003 Nanolithography based on real-time electrically controled indentation with an atomic force microscope for nanocontact elaboration *Nano Lett.* **3** 1599
[66] Bernand-Mantel A, Seneor P, Lidgi N, Munoz M, Cros V, Fusil S, Bouzehouane K, Deranlot C, Vaures A, Petroff F and Fert A 2006 Evidence for spin injection in a single metallic nanoparticle: a step towards nanospintronics *Appl. Phys. Lett.* **89** 062502
[67] Bernand-Mantel A, Seneor P and Petroff F *et al* private communication
[68] Bergmann G 1984 Weak localization in thin films *Phys. Rep.* **107** 1
[69] Gougam A B, Pierre F, Pothier D, Esteve H and Birge N O 2000 Comparison of energy and phase relaxation in metallic wires *J. Low Temp. Phys.* **118** 447
[70] Bird J P (ed) 2003 *Electron Transport in Quantum Dots* (Berlin: Springer)
[71] Elzerman J M *et al* 2005 *Quantum Dots: A Doorway to Nanoscale Physics* (*Lecture Notes in Physics* vol 667) (Berlin: Springer) p 25
[72] Brataas A, Hirano M, Inoue J, Nazarov Y V and Bauer G E W 2001 Spin accumulation in a quantum cluster resolved in tunnel junctions *Japan. J. Appl. Phys.* **40** 2329
[73] Barnaś J, Martinek J, Michałek G, Bułka B R and Fert A 2000 Spin effects in ferromagnetic single-electron transistors *Phys. Rev.* B **62** 12363
[74] Fransson J, Eriksson O and Sandalov I 2002 Many-body approach to spin-dependent transport in quantum dot systems *Phys. Rev. Lett.* **88** 226601
[75] Bułka B R 2000 Current and power spectrum in a magnetic tunnel device with an atomic-size spacer *Phys. Rev.* B **62** 1186
[76] Rudziński W and Barnaś J 2001 Tunnel magnetoresistance in ferromagnetic junctions: tunneling through a single discrete level *Phys. Rev.* B **64** 085318
[77] Weymann I, Barnas J, Konig J, Martinek J and Schon G 2005 Zero-bias anomaly in cotunnelling transport through quantum dot spin valves *Phys. Rev.* B **72** 113301
[78] Weymann I, Konig J, Martinek J, Barnas J and Schon G 2005 Tunnel magnetoresistance of quantum dots coupled to ferromagnetic leads in the sequential and cotunneling regimes *Phys. Rev.* B **72** 115334
[79] Gorelik L Y, Kulinich S I, Shekhter R I, Jonson M and Vinokur V M 2005 Coulomb promotion of spin-dependent tunneling *Phys. Rev. Lett.* **95** 116806
[80] Weymann I and Barnas J 2006 Effect of intrinsic spin relaxation on the spin-dependent cotunneling transport through quantum dots *Phys. Rev.* B **73** 205309
[81] Bułka B R, Martinek J, Michałek G and Barnaś J 1999 Shot noise in ferromagnetic single-electron tunneling devices *Phys. Rev.* B **60** 12246
[82] Cottet A, Belzig W and Bruder C 2004 Positive cross correlations in a three-terminal quantum dot with ferromagnetic contacts *Phys. Rev. Lett.* **92** 206801
[83] Cottet A, Belzig W and Bruder C 2004 Positive cross-correlations due to dynamical channel blockade in a three-terminal quantum dot *Phys. Rev.* B **70** 115315
[84] Mu H-F, Su G and Zheng Q-R 2006 Spin current and current-induced spin transfer torque in ferromagnet–quantum dot–ferromagnet coupled systems *Phys. Rev.* B **73** 054414
[85] Usaj G and Baranger H U 2001 Mesoscopic tunneling magnetoresistance *Phys. Rev.* B **63** 184418
[86] Konig J and Martinek J 2003 Interaction-driven spin precession in quantum-dot spin valves *Phys. Rev. Lett.* **90** 166602
[87] Braun M, Konig J and Martinek J 2004 Theory of transport through quantum-dot spin valves in the weak-coupling regime *Phys. Rev.* B **70** 195345
[88] Rudzinski W, Barnas J, Swirkowicz R and Wilczynski M 2005 Spin effects in electron tunneling through a quantum dot coupled to noncollinearly polarized ferromagnetic leads *Phys. Rev.* B **71** 205307
[89] Braig S and Brouwer P W 2005 Rate equations for Coulomb blockade with ferromagnetic leads *Phys. Rev.* B **71** 195324
[90] Pedersen J N, Thomassen J Q and Flensberg K 2005 Noncollinear magnetoconductance of a quantum dot *Phys. Rev.* B **72** 045341
[91] Gurvitz S A, Mozyrsky D and Berman G P 2005 Coherent effects in magnetotransport through Zeeman-split levels *Phys. Rev.* B **72** 205341

[92] Weymann I and Barnas J 2005 Cotunnelling through quantum dot coupled to ferromagnetic leads with noncollinear magnetizations *Eur. Phys. J.* B **46** 289
[93] Wunderlich J, Jungwirth T, Kaestner B, Irvine A C, Shick A B, Stone N, Wang K-Y, Rana U, Giddings A D, Foxon C T, Campion R P, Williams D A and Gallagher B L 2006 Coulomb blockade anisotropic magnetoresistance effect in a (Ga, Mn)As single-electron transistor *Phys. Rev. Lett.* **97** 077201
[94] Wunderlich J 2004 private communication
[95] Sahoo S, Kontos T, Furer J, Hoffmann C, Graber M, Cottet A and Schonenberger C 2005 Electric field control of spin transport *Nat. Phys.* **1** 1
[96] Venema L C, Wildoer J W G, Janssen J W, Tans S J, Temminck Tuinstra H L J, Kouwenhoven L P and Dekker C 1999 Imaging electron wave functions of quantized energy levels in carbon nanotubes *Science* **283** 52
[97] Tans S J, Devoret M H, Dai H, Thess A, Smalley R E, Geerligs L J and Dekker C 1997 Individual single-wall carbon nanotubes as quantum wires *Nature* **386** 474
[98] Cobden D H, Bockrath M, McEuen P L, Rinzler A G and Smalley R E 1998 Spin splitting and even-odd effects in carbon nanotubes *Phys. Rev. Lett.* **81** 681–4
[99] Cobden D H and Nygård J 2002 Shell filling in closed single-wall carbon nanotube quantum dots *Phys. Rev. Lett.* **89** 046803
[100] Liang W, Bockrath M and Park H 2002 Shell filling and exchange coupling in metallic single-walled carbon nanotubes *Phys. Rev. Lett.* **88** 126801
[101] Kong J, Yenilmez E, Tombler T W, Kim W, Dai H, Laughlin R B, Liu L, Jayanthi C S and Wu S Y 2001 Quantum interference and ballistic transmission in nanotube electron waveguides *Phys. Rev. Lett.* **87** 106801
[102] Liang W, Bockrath M, Bozovic D, Hafner J H, Tinkham M and Park H 2001 Fabry–Perot interference in a nanotube electron waveguide *Nature* **411** 665
[103] Alphenaar B W, Tsukagoshi K and Ago H 1999 Coherent transport of electron spin in a ferromagnetically contacted carbon nanotube *Nature* **401** 572
[104] Zhao B, Monch I, Vinzelberg H, Muhl T and Schneidera C M 2002 Spin-coherent transport in ferromagnetically contacted carbon nanotubes *Appl. Phys. Lett.* **80** 3144
[105] Kim J-R, So H M, Kim J-J and Kim J 2002 Spin-dependent transport properties in a single-walled carbon nanotube with mesoscopic Co contacts *Phys. Rev.* B **66** 233401
[106] Hueso L E, Burnell G, Prieto J L, Granja L, Bell C, Kang D J, Chhowalla M, Cha S N, Jang J E, Amaratunga G A J and Mathur N D 2006 Electrical transport between epitaxial manganites and carbon nanotubes *Appl. Phys. Lett.* **88** 083120
[107] Man H T, Wever I J W and Morpurgo A F 2006 Spin-dependent quantum interference in single-wall carbon nanotubes with ferromagnetic contacts *Phys. Rev.* B **73** 241401
[108] Jensen A, Hauptmann J R, Nygrd J and Lindelof P E 2005 Magnetoresistance in ferromagnetically contacted single-wall carbon nanotubes *Phys. Rev.* B **72** 035419
[109] Nagabhirava B, Bansal T, Sumanasekera G U, Alphenaar B W and Liu L 2006 Gated spin transport through an individual single wall carbon nanotube *Appl. Phys. Lett.* **88** 023503
[110] Javey A, Guo J, Wang Q, Lundstrom M and Dai H 2003 Ballistic carbon nanotube field-effect transistors *Nature* **424** 654
[111] Glazman L and Raikh M E 1988 Resonant Kondo transparency of a barrier with quasilocal impurity states *JETP Lett.* **47** 452
[112] Ng T K and Lee P A 1988 On-site Coulomb repulsion and resonant tunneling *Phys. Rev. Lett.* **61** 1768
[113] Pustilnik M and Glazman L 2004 Kondo effect in quantum dots *J. Phys.: Condens. Matter* **16** R513
[114] Sergueev N, Sun Q-F, Guo H, Wang B G and Wang J 2002 Spin-polarized transport through a quantum dot: Anderson model with on-site Coulomb repulsion *Phys. Rev.* B **65** 165303
[115] Zhang P, Xue Q-K, Wang Y and Xie X C 2002 Spin-dependent transport through an interacting quantum dot *Phys. Rev. Lett.* **89** 286803
[116] Martinek J, Utsumi Y, Imamura H, Barnas J, Maekawa S, Konig J and Schon G 2003 Kondo effect in quantum dots coupled to ferromagnetic leads *Phys. Rev. Lett.* **91** 127203
[117] Bulka B R and Lipinski S 2003 Coherent electronic transport and Kondo resonance in magnetic nanostructures *Phys. Rev.* B **67** 024404
[118] Lopez R and Sanchez D 2003 Nonequilibrium spintronic transport through an artificial Kondo impurity: conductance, magnetoresistance, and shot noise *Phys. Rev. Lett.* **90** 116602
[119] Martinek J, Sindel M, Borda L, Barnas J, Konig J, Schon G and von Delft J 2003 Kondo effect in the presence of itinerant-electron ferromagnetism studied with the numerical renormalization group method *Phys. Rev. Lett.* **91** 247202

[120] Swirkowicz R, Barnas J and Wilczynski M 2003 Nonequilibrium Kondo effect in quantum dots *Phys. Rev.* B **68** 195318
[121] Choi M-S, Sanchez D and Lopez R 2004 Kondo effect in a quantum dot coupled to ferromagnetic leads: a numerical renormalization group analysis *Phys. Rev. Lett.* **92** 056601
[122] Utsumi Y, Martinek J, Schon G, Imamura H and Maekawa S 2005 Nonequilibrium Kondo effect in a quantum dot coupled to ferromagnetic leads *Phys. Rev.* B **71** 245116
[123] Swirkowicz R, Wilczynski M, Wawrzyniak M and Barnas J 2006 Kondo effect in quantum dots coupled to ferromagnetic leads with noncollinear magnetizations *Phys. Rev.* B **73** 193312
[124] Sanchez D and Lopez R 2005 Three-terminal transport through a quantum dot in the Kondo regime: conductance, dephasing, and current–current correlations *Phys. Rev.* B **71** 035315
[125] Martinek J, Sindel M, Borda L, Barnas J, Bulla R, Konig J, Schon G, Maekawa S and von Delft J 2005 Gate-controlled spin splitting in quantum dots with ferromagnetic leads in the Kondo regime *Phys. Rev.* B **72** 121302
[126] Tanaka Y and Kawakami N 2005 Interference effects on Kondo-assisted transport through double quantum dots *Phys. Rev.* B **72** 085304
[127] Sanchez D, Lopez R and Choi M S 2005 Spintronic transport and Kondo effect in quantum dots *J. Supercond.* **18** 251
[128] Jamet M, Wernsdorfer W, Thirion C, Mailly D, Dupuis V, Mélinon P and Pérez A 2001 Magnetic anisotropy of a single cobalt nanocluster *Phys. Rev. Lett.* **86** 4676
[129] Canali C M and MacDonald A H 2000 Theory of tunneling spectroscopy in ferromagnetic nanoparticles *Phys. Rev. Lett.* **85** 5623
[130] Kleff S, von Delft J, Deshmukh M M and Ralph D C 2001 Model for ferromagnetic nanograins with discrete electronic states *Phys. Rev.* B **64** 220401
[131] Kleff S and von Delft J 2002 Nonequilibrium excitations in ferromagnetic nanoparticles *Phys. Rev.* B **65** 214421
[132] Waintal X and Brouwer P W 2003 Tunable magnetic relaxation mechanism in magnetic nanoparticles *Phys. Rev. Lett.* **91** 247201
[133] Inoue J and Brataas A 2004 Magnetization reversal induced by spin accumulation in ferromagnetic transition-metal dots *Phys. Rev.* B **70** 140406
[134] Waintal X and Parcollet O 2005 Current-induced spin torque in a nanomagnet *Phys. Rev. Lett.* **94** 247206
[135] Jalil M B A and Tan S G 2005 Spin transfer and current-induced switching in a ferromagnetic single-electron transistor *Phys. Rev.* B **72** 214417
[136] Parcollet O and Waintal X 2006 Spin torque in a nanomagnet coupled to noncollinear ferromagnetic electrodes *Phys. Rev.* B **73** 144420
[137] Rocha A R, Garcia-Suarez V M, Bailey S W, Lambert C J, Ferrer J and Sanvito S 2005 Towards molecular spintronics *Nat. Mater.* **4** 335
[138] Xiong Z H, Wu D, Vardeny Z V and Shi J 2002 Giant magnetoresistance in organic spin valves *Nature* **427** 821
[139] Thomas L, Lionti F, Ballou R, Gatteschi D, Sessoli R and Barbara B 1996 Macroscopic quantum tunneling of magnetization in a single crystal of nanomagnets *Nature* **383** 145
[140] Friedman J R, Sarachik M P, Tejada J and Ziolo R 1996 Macroscopic measurement of resonant magnetization tunneling in high-spin molecules *Phys. Rev. Lett.* **76** 3830
[141] Wernsdorfer W and Sessoli R 1999 Quantum phase interference and parity effects in magnetic molecular clusters *Science* **284** 133
[142] Kim G-H and Kim T-S 2004 Electronic transport in single-molecule magnets on metallic surfaces *Phys. Rev. Lett.* **92** 137203
[143] Romeike C, Wegewijs M R, Hofstetter W and Schoeller H 2006 Quantum-tunneling-induced Kondo effect in single molecular magnets *Phys. Rev. Lett.* **96** 196601
[144] Heersche H B, deGroot Z, Folk J A, vander Zant H S J, Romeike C, Wegewijs M R, Zobbi L, Barreca D, Tondello E and Cornia A 2006 Electron transport through single Mn12 molecular magnets *Phys. Rev. Lett.* **96** 206801